PRODUCTION ENGINEERING ARCHIVES 2022, 28(4), 375-380

PRODUCTION ENGINEERING ARCHIVES

ISSN 2353-5156 (print)
ISSN 2353-7779 (online)

Exist since 4th quarter 2013
Available online at https://pea-journal.eu

Mathematical modeling of the stress-strain state of the annular preventer seal using the theory of reinforced shells

Jaroslav Grydzhuk[1], Ihor Chudyk[1], Orest Slabyi[1], Yurii Mosora[1,*], Mariana Kovbaniuk[1], Marek Krynke[2]

[1] Ivano-Frankivsk National Technical University of Oil and Gas, 15 Karpatska st., 76019, Ukraine; jaroslav.gridzhuk@gmail.com (JG); ihor.chudyk@nung.edu.ua (IC); burewisnyk@gmail.com (OS); yuramosora@gmail.com (JM); mariannakovbanyuk@gmail.com (MK)
[2] Czestochowa University of Technology, Al. Armii Krajowej 19b, 42-200 Częstochowa, Poland; marek.krynke@wz.pcz.pl
*Correspondence: yuramosora@gmail.com; Tel.: + 380958601575

Article history
Received 17.08.2022
Accepted 28.09.2022
Available online 26.10.2022

Keywords
annular preventer
reinforced shell
combined rubber-metal seal
stress-strain condition

Abstract
Management of wells in the process of their construction is one of the important factors in ensuring the safety of the technological process. Blowout equipment, which includes annular preventers, is used to control the wells. This applies to the construction of oil and gas wells, or wells that provide degassing of coal seams to reduce their gas-dynamic activity. For the purpose of safe and long-term operation of annular preventers on the basis of the theory of thick-walled combined reinforced shells and the carried-out analytical research, the mathematical model for research of a stress-strain condition of a seal of an annular preventer has been offered. Taking into consideration the real design, the seal of the annular preventer is modeled by a rubber shell, reinforced in the circular direction by rubber frames, and in the longitudinal direction by metal stringers. The mathematical model provides for determining the stiffness, internal force factors and stresses in the longitudinal and transverse sections of the combined rubber-metal seal, considering the peculiarities of its operation. At the same time, the model includes the conditions of interaction of the rubber base of the seal with a pipe, as well as the action of sealing pressure under operating conditions. The use of the proposed mathematical model reduces the costs of experimental research and will contribute to ensuring the reliability of simulation modeling results. The advantage of the method is the determination of calculated loads at different points of the combined seal under the existing state of dangerous zones and the influence of operating conditions. In the meantime, prerequisites have been created for expanding the possibilities of simulation modeling and designing structural elements of annular preventers with increased operational characteristics. The practical value of the obtained results is determined by the possibility of using them to ensure the performance of the rubber-metal seal both at the stage of its design and during the operation.

DOI: 10.30657/pea.2022.28.46 JEL: L69 M11

1. Introduction

In various areas of modern technology, such designs are widely used, in which the load-bearing bodies are plates or plate packs. For example, we can cite plate springs, springs, shells reinforced with annular and longitudinal ribs. The use of pack plates and ribs in such a structure is relevant, because it makes it possible to reduce the mass and rigidity of the structure, while maintaining its strength (Yasnii et al., 2020; Belica et al., 2011). The rubber-metal seal of the ring preventer shown in the Figure 1 can be regarded as an example of a shell reinforced with longitudinal steel ribs.

At present, there are known distinct theoretical and experimental studies concerning the design and operation of annular preventers. However, the results of these studies are insufficient for the implementation of a systematic approach to the development and development of reliable designs of annular preventer seals (Hui et al., 2016; Sexsmith, 2018; Mark Allen Group, 2018). First of all, there is no a scientifically based methodology for calculating the geometric and power parameters of the annular preventer and seal unit, which would ensure the sealing ability of preventers of all standard sizes. The effect of the geometry of the seal armature on the stress-deformed state of the seal rubber has not been studied yet (Zhang et al., 2014).

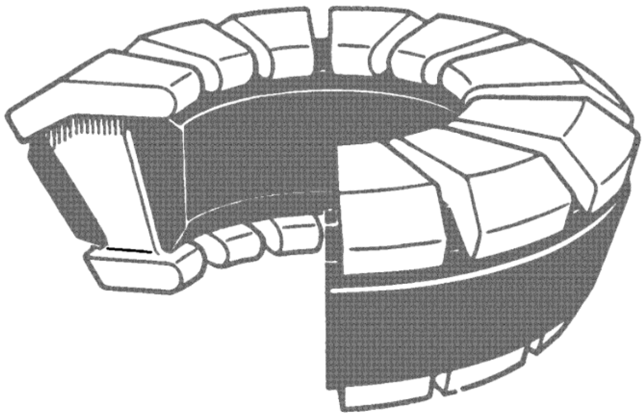

Fig. 1. Annular preventer seal

Mechanical-mathematical modeling of the behavior of non-shearing bodies of these structures under loading conditions lead, at the first stage, to the setting and solving problems for bending packages of plates (ribs), factoring out the internal and external force factors of the mechanical system at the interfaces (Ugural, A.C., 2017; Ciarlet, P.G., 2021).

2. Literature review

Formulations and methods of solving problems considering the contact loads, using continuous models of continuous medium, are quite developed. Among them, the method of singular integral equations, the variational-difference method, the apparatus of variational inequalities, etc., are common (Kanwal and Ram, 2000; Matsuo and Takayasu, 2010). Among others, these methods make it possible to establish the fundamental dependences of the frictional contact of elastic bodies and to solve specific problems. Fundamental results of suggested research direction are highlighted in the works (Yasnii et al., 2020; Zubko et al., 2001; Yasnii et al., 2016; Avramov et al., 2015). At the same time, research using the mentioned methods distinguishes the cumbersomeness of the mathematical apparatus, which increases even more when taking into account anisotropy, as well as the absence of analytical solutions. Therefore, the search for new methods of solving contact problems that can simulate the anisotropy of the physical and mechanical properties of the structure and meet the needs of engineering practice remains relevant.

At present, there is a sufficient number of refined theories of shells, plates and rods capable of counting the effects of transverse shear and crimping, which allow to obtain the distribution of contact stresses without physical correspondences (Yasnii et al., 2016; Avramov et al., 2015; Shengshan et al., 2020; Su et al., 2017). However, the analysis of the existing non-classical theories of shells and plates shows that in most of them the main attention is paid to the study of the effects of transverse shear (Zubko et al., 2001; Avramov et al., 2015; Su et al., 2017. There are also models that pay heed to transverse compression, in particular (Shengshan et al., 2020; Zhong et al., 2017; Tsyss et al., 2016). However, the latter are basically not suitable for solving the contact problems of bending packages of the transversely isotropic plates.

The problem of determining contact stresses in the problems of the theory of shells, plates and rods in most cases is reduced to the solution of integral equations, and often by numerical methods (Yasni et al., 2020; Zhong et al., 2017; Tsyss et al., 2016; Dzhus et al., 2018; Reddy, 2006). The same problem is solved in another way, using a method that is somewhat less frequently but also provides an opportunity to obtain satisfactory results. Here, the problem of determining contact stresses is reduced to the solution of differential equations. Such an approach was implemented in (Yasnii et al., 2016; Shengshan et al., 2020; Su et al., 2017), where in the case of plates with the same mechanical and geometric parameters in the absence of frictional forces on the surfaces of the part, a general analytical solution of the system of differential equations and dependencies for contact stresses in packages with an arbitrary number of plates was obtained.

3. Experimental

The problem of modeling the stress-strain state of the preventer seal can be reduced to the calculation of a cylindrical rubber-metal shell with a base 1, reinforced with annular ribs – frames 2 and longitudinal ribs – stringers 3 (Fig. 2).

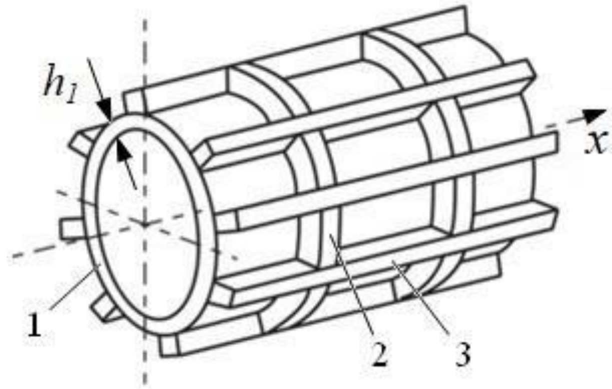

Fig. 2. Initial scheme of the shell reinforced with narrow frames (1-base, 2-frame, 3-stringer)

4. Results and discussion

At the first stage of modeling, we consider a rubber cylindrical shell of constant thickness, which is under the action of axisymmetric loads. The differential equation for the case of a radial deflection of a closed circular cylindrical rubber shell loaded with uniform radial pressure in accordance with [10] has the following form:

$$\boldsymbol{D_1 \frac{d^4 w_1}{dx^4} + \frac{E_1 h_1}{a^2} w_1 = q_1;} \quad (1)$$

where:

$\boldsymbol{w_1(x)}$ – radial movement of the points of the middle surface of the shell;

$\boldsymbol{a}$ – the radius of the middle surface of the rubber shell;

$\boldsymbol{h_1}$ – thickness of the wall of the rubber shell;

$\boldsymbol{E_1}$ – modulus of elasticity of the rubber shell;

$\boldsymbol{\mu_1}$ – Poisson's ratio for the rubber shell;

$\boldsymbol{q_1}$ – distributed load applied to the middle surface of the shell;

$\boldsymbol{D_1}$ – cylindrical rigidity of the shell;

$$\boldsymbol{D_1 = \frac{E_1 h_1^3}{12(1-\mu_1^2)}}. \tag{2}$$

Giving thoughtful attention to the real design of the annular preventer seal, the model (Fig. 2) has been abstracted to the following state: the shell rubber is left, and all the cavities between the stringers will be replaced by rubber frames, the width of each will be equal to the length of the stringer. As a result, we will get a combined orthotropic rubber shell reinforced in the longitudinal direction by thin metal stringers (Fig. 3). Let's determine to which class the shell under the investigation belongs. Since more than 90% of its volume is occupied by rubber, we will be guided by the parameters of the rubber shell. A detailed investigation of this question shows that a shell can be considered as a long one if the shell parameter $\beta_1 l_1 \geq 3$; where $\beta_1 = = \sqrt[4]{\frac{3(1-\mu_1^2)}{(ah_1)^2}}$ – displacement damping coefficient, which shows how much the displacements are damped with the distance from the place of application of the load. Based on actual design dimensions $a = 0{,}11\text{м}$; $h_1 = 0{,}04\text{м}$; $l_1 = 0{,}2$; $\mu_1 = 0{,}47$ we get $\beta_1 l_1 = 3{,}7$; which gives a reason to consider the shell to be long. However, reducing l_1, or increasing the thickness of h_1 by one and a half times, automatically transfers the shell to the short class.

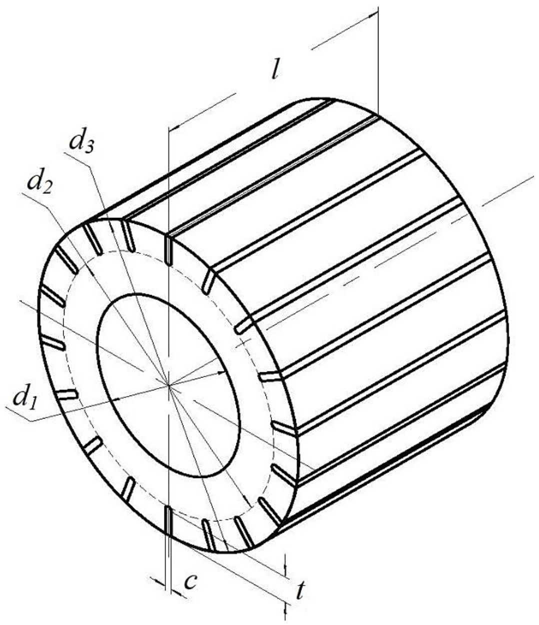

Fig. 3. Calculation scheme of a reinforced shell with wide frames

At the second stage of modeling, the critical axial load of the combined shell with symmetric and asymmetric buckling of the rubber base of the seal has been characterized. The distributed load applied to the middle surface of the rubber shell of the seal will correspond to the contact pressure between the pipe and the seal, which will be determined from the ratio:

$$\boldsymbol{q_1 = p_s tg\alpha}; \tag{3}$$

where:

$\boldsymbol{\alpha}$ – the taper angle of the seal;

$\boldsymbol{p_s}$ – sealing pressure (pressure on the outer surface of the seal from the side of the plunger).

Taking into account the design features of the combined rubber-metal shell (Fig. 2) according to (Byrher et al., 1966), the critical value of the contact pressure on the outer surface of the seal, as well as the axial load during symmetrical and asymmetrical buckling, can be estimated by the following dependencies, respectively:

$$\boldsymbol{q_{cr} = \frac{5{,}4\sqrt[4]{A_x}\sqrt[4]{D_\varphi^3}}{lR\sqrt{R}}}; \tag{4}$$

$$\boldsymbol{P_{cr}^{sym} = 4\pi(1-\mu_1^2)\sqrt{A_\varphi D_x}}; \tag{5}$$

$$\boldsymbol{P_{cr}^{asym} = 4\pi(1-\mu_1^2)\sqrt{A_x D_\varphi}}; \tag{6}$$

where:

$\boldsymbol{A_x}$, $\boldsymbol{A_\varphi}$ – tensile stiffness of the shell in the longitudinal and circumferential directions, respectively;

$$\boldsymbol{A_x = \frac{E_1 h_1}{1-\mu_1^2} + \frac{E_3 F_3}{l_3}}; \tag{7}$$

$$\boldsymbol{A_\varphi = \frac{E_1 h_1}{1-\mu_1^2} + \frac{E_2 F_2}{l_2}}; \tag{8}$$

$\boldsymbol{D_x}$, $\boldsymbol{D_\varphi}$ – bending stiffness in the longitudinal and circular directions, respectively;

$$\boldsymbol{D_x = \frac{E_1 h_1^3}{12(1-\mu_1^2)} + \frac{E_3 J_3}{l_3} - \frac{E_1 b_3 h_1^3}{12 l_3}}; \tag{9}$$

$$\boldsymbol{D_\varphi = \frac{E_1 h_1^3}{12(1-\mu_1^2)} + \frac{E_2 J_2}{l_2} - \frac{E_1 b_2 h_1^3}{12 l_2}}; \tag{10}$$

where:

$\boldsymbol{E_3}$; $\boldsymbol{E_2}$ – modulus of elasticity of metal stringer and rubber frame, respectively;

$\boldsymbol{F_3}$; $\boldsymbol{F_2}$ – the cross-sectional area of the metal stringer and the rubber frame, respectively;

$\boldsymbol{J_3}$; $\boldsymbol{J_2}$ – the moment of inertia of the cross-section of the metal stringer and the rubber frame, respectively;

$\boldsymbol{l_3 = \frac{2\pi R}{N_3}}$ – the distance between the centers of mass of the cross sections of two adjacent metal stringers;

$\boldsymbol{N_3}$ – number of metal stringers;

$\boldsymbol{l_2}$ – the coordinate of the center of mass of the rubber frame in the longitudinal direction, $\boldsymbol{l_2 = \frac{l}{2}}$;

$\boldsymbol{l}$ – length of the rubber-metal shell (stringer length);

$\boldsymbol{b_2}$ – the width of the intercostal rubber frame on the middle surface;

$\boldsymbol{d_1}$ – the inner diameter of the combined shell;
$\boldsymbol{d_2}$ – the median diameter of the combined shell;
$\boldsymbol{d_3}$ – outer diameter of the combined shell;
$\boldsymbol{R} = \frac{(d_2-d_1)}{2}$ – the radius of the middle surface of the rubber base of the combined shell;
c, $\boldsymbol{t}$ – respectively, the width and height of the cross section of the steel stringer.

In the course of experimental studies (Mykhailiuk et al., 2021), the values of the loads applied to the natural model with inserts with a width of 30 and 40 mm have been established. They were 59 and 66 kN, respectively. As shown by the results of simulation modeling of the stress-strain state of the same full-scale model (Mykhailiuk et al., 2021), the inner surface (rubber base) of the rubber-metal seal experiences the greatest radial movements and corresponding contact loads. Therefore, it makes sense to develop an analytical unit for studying the parameters of the stress-strain state of the rubber-metal seal and compare the results with the experimental ones.

At the third stage of modeling, we will describe the internal force factors acting on a unit length of the rubber base. Considering the possibility of relative radial movement of the points of the inner surface of the combined shell during crimping and its design features, we believe that the ends of the rubber shell will have hinged fasteners at the edges (**Fig. 2**), which will meet the following boundary conditions: $\boldsymbol{x} = \boldsymbol{0}$; $\boldsymbol{w}(\mathrm{x}) = \boldsymbol{0}$; $\boldsymbol{w}''(\mathrm{x}) = \boldsymbol{0}$. For a long rubber shell, the solution of equation (1) according to (Byrher et al., 1966) in the absence of heating is written as a function of radial movements of the middle surface:

$$\boldsymbol{w_1}(\boldsymbol{x}) = \frac{q_1 a_1^2}{E_1 h_1}\left[\boldsymbol{1} - \boldsymbol{e^{-k_1 x}c(\beta_1 x)}\ \right]; \quad (11)$$

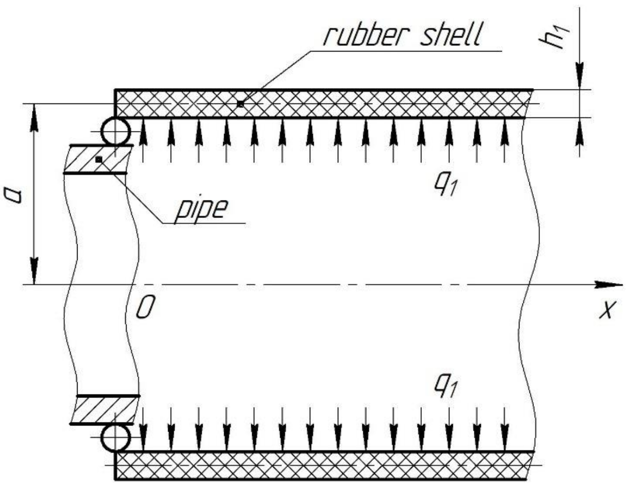

Fig. 4. The calculation scheme of the hinged contact of the end of the shell with the pipe

By differentiating function (3) three times along the x coordinate, we get:

$$\frac{dw(x)}{dx} = \frac{2\beta_1 q_1 a_1^2}{E_1 h_1} e^{-\beta_1 x}(\boldsymbol{cos\,cos\,(\beta_1 x)}\ + \boldsymbol{sin\,sin\,(\beta_1 x)}\,); \quad (12)$$

$$\frac{d^2w(x)}{dx^2} = -\frac{2\beta_1^2 q_1 a_1^2}{E_1 h_1} e^{-\beta_1 x}\,\boldsymbol{sin\,sin\,(\beta_1 x)}\,; \quad (13)$$

$$\frac{d^3w(x)}{dx^3} = -\frac{2\beta_1^3 q_1 a_1^2}{E_1 h_1} e^{-\beta_1 x}(\boldsymbol{cos\,cos\,(\beta_1 x)}\ - \boldsymbol{sin\,sin\,(\beta_1 x)}\,); \quad (14)$$

Concentrated transverse force:

$$\boldsymbol{Q} = \boldsymbol{D_\varphi}\frac{d^3 w_1(x)}{dx^3}; \quad (15)$$

or with consideration (10) and (14)

$$\boldsymbol{Q} = \left[\frac{E_1 h_1^3}{12(1-\mu_1^2)} + \frac{E_2 J_2}{l_2} - \frac{E_1 b_2 h_1^3}{12 l_2}\right] e^{-\beta_1 x}(\boldsymbol{cos\,cos\,(\beta_1 x)}\ - \boldsymbol{sin\,sin\,(\beta_1 x)}\,) \quad (16)$$

Concentrated longitudinal force:

$$\boldsymbol{N} = \boldsymbol{E_1 h_1}\frac{w_1(x)}{a} \quad (17)$$

or with consideration (11)

$$\boldsymbol{N} = \boldsymbol{q_1 a_1}\left[\boldsymbol{1} - \boldsymbol{e^{-k_1 x}c(\beta_1 x)}\ \right] \quad (18)$$

Bending moment in cross section:

$$\boldsymbol{M_x} = \boldsymbol{D_x}\frac{d^2 w_1(x)}{dx^2}; \quad (19)$$

or with consideration (9) and (13)

$$\boldsymbol{M_x} = \left[\frac{E_1 h_1^3}{12(1-\mu_1^2)} + \frac{E_3 J_3}{l_3} - \frac{E_1 b_3 h_1^3}{12 l_3}\right] e^{-\beta_1 x}\,\boldsymbol{sin\,sin\,(\beta_1 x)}\,; \quad (20)$$

Bending moment in longitudinal section:

$$\boldsymbol{M_\varphi} = \boldsymbol{D_\varphi \mu_1}\frac{d^2 w_1(x)}{dx^2}; \quad (21)$$

or with consideration (10) and (13)

$$\boldsymbol{M_\varphi} = \left[\frac{E_1 h_1^3}{12(1-\mu_1^2)} + \frac{E_2 J_2}{l_2} - \frac{E_1 b_2 h_1^3}{12 l_2}\right] e^{-\beta_1 x}\,\boldsymbol{sin\,sin\,(\beta_1 x)}\,; \quad (22)$$

Bending stress in the cross section:

$$\sigma_x = -\frac{12 M_x z}{h_1^3}; \quad (23)$$

or with consideration (16)

$$\sigma_x = -\frac{12z}{h_1^3}\left[\frac{E_1 h_1^3}{12(1-\mu_1^2)} + \frac{E_3 J_3}{l_3} - \frac{E_1 b_3 h_1^3}{12 l_3}\right] e^{-\beta_1 x}\,\boldsymbol{sin\,sin\,(\beta_1 x)}\,; \quad (24)$$

Bending stress in the longitudinal section:

$$\sigma_\varphi = -\frac{12 M_\varphi z}{h_1^3}; \quad (25)$$

or with consideration (18)

$$\sigma_\varphi = -\frac{12z}{h_1^3}\left[\frac{E_1 h_1^3}{12(1-\mu_1^2)} + \frac{E_2 J_2}{l_2} - \frac{E_1 b_2 h_1^3}{12 l_2}\right] e^{-\beta_1 x}\,\boldsymbol{sin\,sin\,(\beta_1 x)}\,; \quad (26)$$

where:
$\boldsymbol{z} = \pm\frac{h_1}{2}$ – the distance from the point to the middle surface of the shell; "+" – for external, "–" – for the inner layer of the shell.

Tangential stress in the cross section:

$$\boldsymbol{\tau} = \frac{Q}{h}\left(\frac{3}{2} - \frac{6z^2}{h^2}\right); \quad (27)$$

or with consideration (16)

$$\tau = \frac{1}{h}\left(\frac{3}{2} - \frac{6z^2}{h^2}\right)\left[\frac{E_1 h_1^3}{12(1-\mu_1^2)} + \frac{E_2 J_2}{l_2} - \frac{E_1 b_2 h_1^3}{12 l_2}\right] e^{-\beta_1 x}(co(\beta_1 x) - si(\beta_1 x)). \tag{28}$$

Normal tensile stresses in the longitudinal section:

$$\sigma_p = \frac{N}{h}; \tag{29}$$

or with consideration (18)

$$\sigma_p = \frac{q_1 a_1[1-e^{-k_1 x} c(\beta_1 x)]}{h_1} \tag{30}$$

Normal stress in the longitudinal section:

$$\sigma_\varphi = \frac{N}{h_1} - \frac{12 M_\varphi z}{h_1^3}; \tag{31}$$

or with consideration (18) and (22)

$$\sigma_\varphi = \frac{q_1 a_1[1-e^{-k_1 x} c(\beta_1 x)]}{h_1} - \frac{12z}{h_1^3}\left[\frac{E_1 h_1^3}{12(1-\mu_1^2)} + \frac{E_2 J_2}{l_2} - \frac{E_1 b_2 h_1^3}{12 l_2}\right] e^{-\beta_1 x} \sin \sin(\beta_1 x). \tag{32}$$

5. Summary and conclusion

The set of obtained analytical dependencies (15)-(32) is a mathematical model for studying the stress-strain state of the combined rubber-metal shell. They make it possible to establish force factors and their corresponding stresses depending on the amount of radial narrowing and the longitudinal coordinate. The graphic interpretation of dependencies (15)-(32) is shown in Fig. 5.

The change in concentrated forces, bending moments and corresponding stresses in the longitudinal and transverse sections is sinusoidal; bending stresses in the longitudinal and transverse sections reach the maximum value of 163 MPa and 77 MPa, respectively, at x = 0.04 m; at the same time, when the maximum normal tensile stress and tangential stress in the cross-section are 127 MPa and 29 MPa, respectively, observed at x = 0.07 m. This feature of the combined rubber-metal shell is explained by its orthotropic properties, which differ along three mutually orthogonal axes of rotational symmetry.

The proposed mathematical model is quite simple and universal, it can be easily implemented on the basis of automated software products MathLAB, Maple, MathCAD. In the future, with its help, it is possible to carry out verification calculations in order to optimize the design of the rubber-metal seal.

Regarding the shortcomings of the developed mathematical model, the following should be highlighted:

1) disregarded in the function of radial movements $w_1(x)$ one more variable - the radius of the middle surface of the base of the rubber-met val shell, which changes in the process of sealing the annular space;

2) the distributed load (contact pressure) q_1 in the connection of the pipe and the combined rubber-metal shell is considered constant, although when the load on the side of the plunger increases, this contact pressure increases, and the radius of its middle surface decreases.

The introduction of the radius of the middle surface as another variable in the function of radial displacement $w_1(x)$ will require the use of partial derivatives in the system of equations (1), which will subsequently lead to the inevitable complication of the formulas for the practical calculation of stresses (15)-(32).

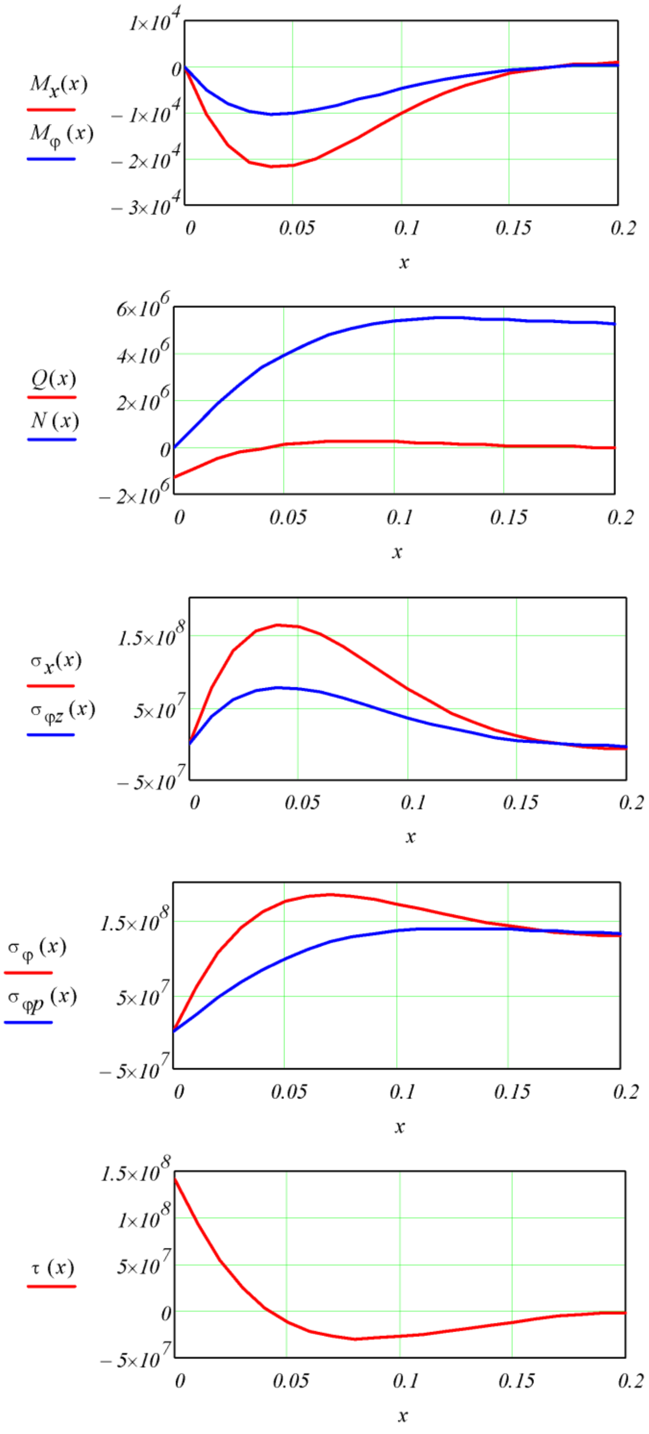

Fig. 5. Graphical dependence of internal force factors and stresses on the longitudinal coordinate of the long shell (d_1 = 170mm; d_3 = 310 mm; l = 250 mm)

The change in pressure q_1 and the corresponding tension in the radial and axial directions is a multifactorial process that depends on the physical and mechanical properties of the rubber-metal shell, the study of which currently requires a significant number of field experiments.

If, due to certain operating factors, there will be a decrease in l_1, or an increase in the thickness of h_1 by one and a half times, it makes sense to establish analytical dependencies for studying the stress-strain state of the short shell.

Reference

Avramov, K.V., Zholos, O.V., 2015. Svobodnyie kolebaniya orebrennyih tonkostennyih tsilindricheskih obtekateley raketonositeley. Visnik NTU "HPI", 55, 13-15.

Belica, T., Malinowski, M., Magnucki, K., 2011. Dynamic Stability of an Isotropic Metal Foam Cylindrical Shell Subjected to External Pressure and Axial Compression. Journal of Applied Mechanics, 78(4), DOI: 10.1115/1.4003768

Byrher, Y.A., Shorr, B.F., Shneiderovych, R.M., 1966. Raschet na prochnost detalei mashyn, M, 616

Ciarlet, P.G., 2021. Mathematical Elasticity: Theory of Shells. Society for Industrial and Applied Mathematics, DOI: 10.1137/1.9781611976823

Daisuke, F., Takayasu, M., 2010. Discrete Variational Derivative Method., Chapman and Hall/CRC, DOI: 10.1201/b10387

Dzhus, A., Andrusyak, A., Grydzhuk, Ja., Romanyshyn, T., 2018. Development of a method for assessing the capacity of equipment for the transportation of compressed natural gas. Eastern-European Journal of Enterprise Technologies, 94, 13-17, ISSN 1729-3774 4/7

Estrada, R., Kanwal, R.P., 2000. Singular Integral Equations., Birkhäuser Boston, DOI: 10.1007/978-1-4612-1382-6

Hui, Y., Yalei, Z., Jianguo, L., Hongyuan J., 2016. Analyses toward factors influencing sealing clearance of a metal rubber seal and derivation of a calculation formula. Chinese Journal of Aeronautics, 29(1), 292-296, DOI: 10.1016/j.cja.2015.09.002

Mark Allen Group, 2018. Metal-to-metal well equipment seal. Sealing Technology, 2018(9), 13, DOI: 10.1016/s1350-4789(18)30377-5

Mykhailiuk, B.B., Chudyk, I.I., Mosora Yu, R., 2021. On the possibility of using simulation modeling for research and design of universal preventer seals. Scientific Bulletin of Ivano-Frankivsk National Technical University of Oil and Gas, 1(50), 53-61, DOI: 10.31471/1993-9965-2021-1(50)-53-61

Reddy, J.N., 2006. Theory and Analysis of Elastic Plates and Shells., CRC Press, DOI: 10.1201/9780849384165

Sexsmith, F.H., 2018. Rubber-to-Metal Bonding. Rubber Products Manufacturing Technology, 449-472, Routledge, DOI: 10.1201/9780203740378-11

Shengshan, P., Muzhou, Z., Bassem, A., Hang, Z., Lian, L., 2020. Compressive behavior of cylindrical rubber buffer confined with fiber reinforced polymer. Journal of Low Frequency Noise, Vibration and Active Control, 39(3), 470-484.

Su, B., Zhou, Z., Xiao, G., Wang, Z., Shu, X., Li, Z., 2017. A pressure-dependent phenomenological constitutive model for transversely isotropic foams, International Journal of Mechanical Sciences, 120, 237-248.

Tsyss, V.G., Sergaeva, M.Yu., 2016. Simulating of the composite cylindrical shell of the pipe of the supply pipelines based on ANSYS package. Procedia Engineering, 152, 332-338.

Ugural, A.C., 2017. Plates and Shells. CRC Press, DOI: 10.1201/9781315104621

Yasnii, P.V., Pyndus, Yu.I., Hud, M.I., 2016. Analiz chastot i form vlasnykh kolyvan pidsylenykh tsylindrychnykh obolonok. Visnyk Ternopilskoho natsionalnoho tekhnichnoho universytetu, 3, 7-15.

Yasnii, P.V., Pyndus, Yu.I., Hud, M.I., 2020. Analysis of the stress-strain state of a reinforced cylindrical shell with free transverse oscillations. Prospecting and Development of Oil and Gas Fields, 4(77), 41-49, DOI: 10.31471/1993-9973-2020-4(77)-41-49

Zhang, Wan-Fu, Yang, Jian-Gang, Li, Chun, Tian, Yong-Wei, 2014. Comparison of leakage performance and fluid-induced force of turbine tip labyrinth seal and a new kind of radial annular seal. Computers & Fluids, 105, 125-137, DOI: 10.1016/j.compfluid.2014.09.010

Zhong, J., Ren, J., Ma. D., 2018. Study on the Deformation and Stress Analysis of the Sponge/Rubber Adapter. Mathematical Problems in Engineering, 117-125.

Zubko, V.I., Shopa, V.M., 2001. Zghyn paketiv transversalno-izotropnykh plastyn. Ivano-Frankivsk, 266.

基于加筋壳理论的环形防喷器密封应力-应变状态数学建模

關鍵詞
环形防喷器
加固外壳
组合橡胶-金属密封
应力应变条件

摘要
井在施工过程中的管理是保证工艺过程安全的重要因素之一。包括环形防喷器在内的防喷设备用于控制油井。这适用于石油和天然气井的建设，或提供煤层脱气以减少其气体动力活动的井。为使环形防喷器安全、长期运行，在厚壁组合加筋壳理论和分析研究的基础上，建立了密封件应力-应变条件数学模型。提供了环形防喷器。考虑到实际设计，环形防喷器的密封采用橡胶壳模型，圆周方向用橡胶框架加强，纵向用金属纵梁加强。考虑到其操作的特性，该数学模型用于确定组合橡胶-金属密封件的纵向和横向截面的刚度、内力因子和应力。同时，该模型包括密封橡胶底座与管道相互作用的条件，以及工作条件下密封压力的作用。所提出的数学模型的使用降低了实验研究的成本，将有助于确保仿真建模结果的可靠性。该方法的优点是确定了在危险区存在状态和运行条件影响下组合密封不同点的计算载荷。与此同时，已经为扩大模拟建模的可能性和设计具有更高运行特性的环形防喷器的结构元件创造了先决条件。所得结果的实用价值取决于使用它们来确保橡胶金属密封件在其设计阶段和运行期间的性能的可能性.